Leptosphaeria rhodopsin: Bacteriorhodopsin-like proton pump from a eukaryote

Stephen A. Waschuk*, Arandi G. Bezerra, Jr.*†, Lichi Shi*, and Leonid S. Brown*‡

*Department of Physics, University of Guelph, Guelph, ON, Canada N1G 2W1; and †Departamento de Fisica, Centro Federal de Educação Tecnológica do Paraná, CEFET-PR 80230-901, Curitiba, Paraná, Brazil

Edited by Robert M. Stroud, University of California, San Francisco, CA, and approved March 30, 2005 (received for review December 22, 2004)

Bacteriorhodopsin-like proteins provide archaea and eubacteria with a unique bioenergetic pathway comprising light-driven transmembrane proton translocation by a single retinal-binding protein. Recently, homologous proteins were found to perform photosensory functions in lower eukaryotes, but no active ion transport by eukaryotic rhodopsins was detected. By demonstrating light-driven proton pumping in a fungal rhodopsin from *Leptosphaeria maculans*, we present a case of a retinal-based proton transporter from a eukaryote. This result implies that in addition to oxidative phosphorylation and chlorophyll photosynthesis, some lower eukaryotes may have retained the archaeal route of building an electrochemical transmembrane gradient of protons.

proton transport | sensory rhodopsins

Since the advent of Mitchell's chemiosmotic theory, two primary means for creating a transmembrane electrochemical gradient of protons ($\Delta\mu_{H^+}$) have been recognized. Both ways are coupled to electron transfer and fall under the broad categories of respiration and chlorophyll-based photosynthesis. About 30 years ago, halophilic archaebacteria were found to possess a different type of photosynthesis, a retinal-based process not coupled to electron transfer, where light-driven translocation of protons is performed by a single membrane protein, bacteriorhodopsin (BR) (1). Recently, it was found that many eubacterial species possess proton-translocating rhodopsins as well, as was first demonstrated for γ-proteobacteria (2). Microbial rhodopsins, also known as rhodopsins of haloarchaeal type, are a class of membrane proteins with seven transmembrane helices surrounding a retinal chromophore, which is covalently linked to a lysine side-chain in the seventh helix via a Schiff base. Photoexcitation drives selective isomerization of the retinal, inducing conformational changes in the protein. Microbial rhodopsins bind all-*trans*-retinal (as opposed to 11-*cis*-retinal-based visual pigments) and have two primary functions, photosensory transduction and light-driven ion transport (3). To date, the ion transport function has only been observed in the archaea and eubacteria, with the function of eukaryotic rhodopsins of haloarchaeal type suggested to be photosensory, as in the fungi *Allomyces reticulatus* and *Neurospora crassa* (4–6). Recently, the photosensory function was demonstrated for the rhodopsins of the alga *Chlamydomonas reinhardtii* (7), where rhodopsin constitutes a light-sensitive domain in a larger membrane protein (7, 8). In this study, we characterize a very different microbial rhodopsin found in the fungal agent of blackleg in canola, *Leptosphaeria maculans* (9, 10). We demonstrate that *Leptosphaeria* rhodopsin (LR) represents a proven case of a proton-pumping retinal protein from a eukaryotic organism. This result suggests that eukaryotes may use the retinal-based bioenergetic pathway previously observed only in prokaryotes.

Materials and Methods

Heterologous Expression of *Leptosphaeria* Rhodopsin. The *L. maculans ops* gene was modified and cloned into the pHIL-S1 vector similarly to the procedure previously used for *Neurospora* rhodopsin (NR) (11). Briefly, *L. maculans ops* was modified such that *Leptosphaeria* opsin was N-terminally truncated (48 residues) with a 6× His-tag added to the C terminus. The protein was expressed in the methylotrophic yeast *Pichia pastoris*, strain GS115, employing our optimized procedure for NR (12). During expression in *P. pastoris*, 5 μM all-*trans*-retinal (Sigma) was added to the growth medium at ≈24 h after induction with methanol. The D150N mutant of LR was produced by a single-step PCR from the wild-type construct and expressed analogously to the wild type.

Isolation, Purification, and Reconstitution of *Leptosphaeria* Rhodopsin. Breakage of *P. pastoris* cells, solubilization of the membranes, and purification and concentration of LR followed our methods previously used for NR (12). *N*-dodecyl-β-D-maltoside treatment of the membranes followed by sequential centrifugations yielded a clear supernatant with membranes containing LR, suitable for optical spectroscopy, that were encased in polyacrylamide gels (6). For reconstitution into liposomes, solubilized Ni-NTA-purified LR was added to preformed liposomes at a ratio of 3:1 lipid/protein (wt/wt) for 1,2-dimyristoyl-*sn*-glycero-3-phosphocholine and 1,2-dimyristoyl-*sn*-glycero-3-phosphate (DMPC:DMPA) liposomes, and 65:1 lipid/protein ratio for L-α-phosphatidylcholine and L-α-phosphatidic acid, L-α-phosphatidylserine, or cardiolipin (PC:PA, PC:PS, PC:CL) liposomes. In the case when the pH-sensitive dye 8-hydroxypyrene-1,3,6-trisulfonic acid trisodium salt (pyranine) had to be entrapped, it was added to the liposomes to a final concentration of 10 mM. Liposome preformation was performed by hydration of the dry lipids, with DMPC:DMPA liposomes at a ratio of 9:1 (wt/wt) and PC:PA (PC:PS, PC:CL) at 4:1 (wt/wt). Reconstitution by detergent (Triton X-100) removal was done using Bio-Beads SM-2 (Bio-Rad), as described in ref. 12. Liposomes were washed repeatedly by centrifugation with 50 mM Na_2SO_4 and 50 mM K_2SO_4 at speeds of 40,000 × *g* (DMPC:DMPA) or 150,000 × *g* (PC:PA, PC:PS, or PC:CL). DMPC:DMPA liposomes were frozen for further use, and PC:PA liposomes were stored at 4°C and used shortly thereafter.

Time-Resolved Laser Spectroscopy in the Visible Range. Time-resolved laser spectroscopy in the visible range was performed on our custom-built apparatus. Photocycle excitation was provided by the second harmonic of a Nd–yttrium/aluminum garnet (YAG) laser (Continuum Minilite II), using ≈7-ns pulses at 532 nm. Absorption changes of monochromatic light (provided by an Oriel QTH source and two monochromators) were followed by using an Oriel photomultiplier with 350-MHz wide-bandwidth amplifier and a Gage analog-to-digital converter (CompuScope 12100-64M). The traces were converted into a quasilogarithmic

This paper was submitted directly (Track II) to the PNAS office.

Abbreviations: BR, bacteriorhodopsin; CL, cardiolipin; DMPC, 1,2-dimyristoyl-*sn*-glycero-3-phosphocholine; DMPA, 1,2-dimyristoyl-*sn*-glycero-3-phosphate; LR, rhodopsin from *Leptosphaeria maculans*; NR, rhodopsin from *Neurospora crassa*; PA, L-α-phosphatidic acid; PC, L-α-phosphatidylcholine; PS, L-α-phosphatidylserine.

‡To whom correspondence should be addressed. E-mail: leonid@physics.uoguelph.ca.

time scale by using homemade software. Global multiexponential analysis of the data were performed as described in ref. 6. The proton kinetics were measured with pyranine on unbuffered suspensions of DMPC:DMPA liposomes, because the LR-containing membranes had high buffering capacity and low protein content. The high protein:lipid ratio of the liposomes made them permeable to protons, removing possible interference with the proton kinetics measurements. The changes followed at 457 nm without pyranine were subtracted from those with pyranine, producing the kinetics for the proton uptake and release.

Vibrational Spectroscopy (Raman and FTIR). Raman spectroscopy was performed as described earlier for NR (12) on DMPC:DMPA liposomes, using a Renishaw Raman imaging microscope (System 2000) with excitation at 785 nm. Light-adaptation of the sample was performed by illumination with a 515-nm laser. Rapid-scan FTIR was performed by using a Bruker IFS66vs machine with a temperature-controlled sample holder (Harrick), and excitation was provided by the second harmonic of a Nd-YAG laser (Continuum Minilite II), using ≈7-ns pulses at 532 nm. Hydrated films of DMPC:DMPA liposomes were compressed between two CaF_2 windows with 2 × 12-μm spacers, and data acquisition was controlled by OPUS software (Bruker).

Proton Transport Measurements. The efficacy of proton transport by LR was studied by using LR reconstituted in PC:PA (PC:PS, PC:CL) liposomes. The low protein:lipid ratio was necessary to ensure tightness of the liposomes. A pH electrode was placed in the liposome suspension, and alkalinization of the medium was measured after illumination with light >550 nm. Alternatively, we measured acidification of the internal volume of the liposomes monitoring changes in the absorption of the trapped pyranine, using two crossed glass filters (>550 nm on the light source and 350–500 nm on the detector) in a Varian Cary 50 Bio UV-visible spectrophotometer.

Results and Discussion

Original analysis of the nucleotide sequence of the *ops* gene of *L. maculans* showed high homology between the putative transmembrane regions of the encoded opsin and those of BR (9). Based on this homology, it was suggested that the *ops* gene product may have a proton-pumping function. We expressed the opsin from *L. maculans* in membranes of the methylotrophic yeast *P. pastoris*, using the protocol developed for *Neurospora* rhodopsin (11, 12). Upon addition of all-*trans*-retinal, a stable red pigment (LR) with an absorption maximum (λ_{max}) of 542 nm was formed in the yeast membranes. The red-shifted λ_{max} of the bound retinal is indicative of a protonated Schiff base linkage, as also evidenced by the position of C=N stretching vibrations (1,648 cm^{-1}) (13) detected by Raman spectroscopy of LR reconstituted into liposomes (Fig. 1). The Raman spectra were markedly BR-like, indicating that the isomeric state of the retinal is predominantly all-*trans*, with a small proportion of 13-*cis*. A large H/D shift of the C=N stretching vibrations (21 cm^{-1}) suggests a strong counterion for the Schiff base (14).

Time-resolved laser spectroscopy in the visible range performed on LR in *P. pastoris* membranes provided information on its photochemical cycle. Global multiexponential analysis of the data shown in Fig. 2 revealed photocycle intermediates resembling the K, L, M, N, and O states of BR (15). Strikingly, the photocycle turnover was very fast (few tens of milliseconds) and the kinetics of the photointermediates had rates similar to those of BR. Slow photocycle kinetics are viewed as a hallmark of photosensory rhodopsins (seconds-long turnover being advantageous for signal transduction), whereas a fast photocycle (<50 ms) is optimal for efficient proton transport

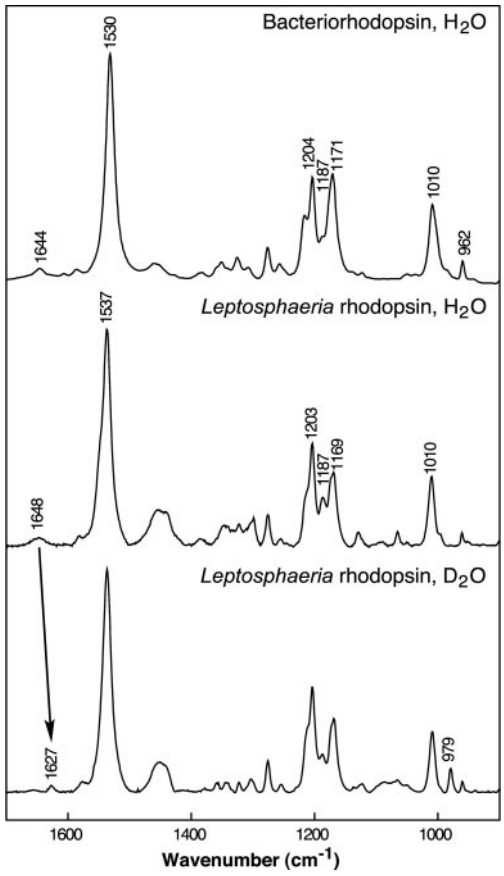

Fig. 1. Preresonance Raman spectra of light-adapted LR (excited at 785 nm) in DMPC:DMPA liposomes hydrated with either H_2O or D_2O. The spectra are strongly dominated by the retinal bands and show the BR-like conformation (predominantly all-*trans*) of the chromophore (the characteristic bands are labeled). The large H/D shift of the C=N stretching vibrations of the protonated Schiff base (from 1,648 to 1,627 cm^{-1}, indicated by arrow) argues for a strong counterion. Spectrum of BR in purple membranes is included for comparison.

(3, 6). Our data would thus suggest that LR may possess proton-pumping ability, in contrast to the slow-cycling fungal rhodopsin from *Neurospora*, NR, which does not transport protons when expressed in *P. pastoris* (6, 11). Furthermore, the photocycle turnover remained fast when LR was reconstituted into PC:PA or DMPC:DMPA liposomes, which suggests that the photocycle in the native system should also maintain its fast character. It should be noted that if LR has a photosensory function, the interactions with a putative transducer may abolish the proton transport, as occurs in haloarchaeal sensory rhodopsins (16). Such interactions may also slow down the photocycle turnover, although halobacterial sensory rhodopsins possess very slow photocycles even in the absence of their transducers.

Further support for a possible proton-transporting function of LR came from studies of the photocycle events related to proton transfers. The LR photocycle exhibited a strong D_2O-dependence (Fig. 3*a*), most notably in the rise and decay of the M- and O-like intermediates (as followed at 420 and 620 nm, respectively), implying that there are proton-transfer steps in the photocycle. To verify the presence of proton uptake and release in the photocycle from/to the external medium we used the pH-sensitive dye pyranine (17). Pyranine measurements in a suspension of proton-permeable DMPC:DMPA proteoliposomes revealed that LR takes up a proton during the M decay

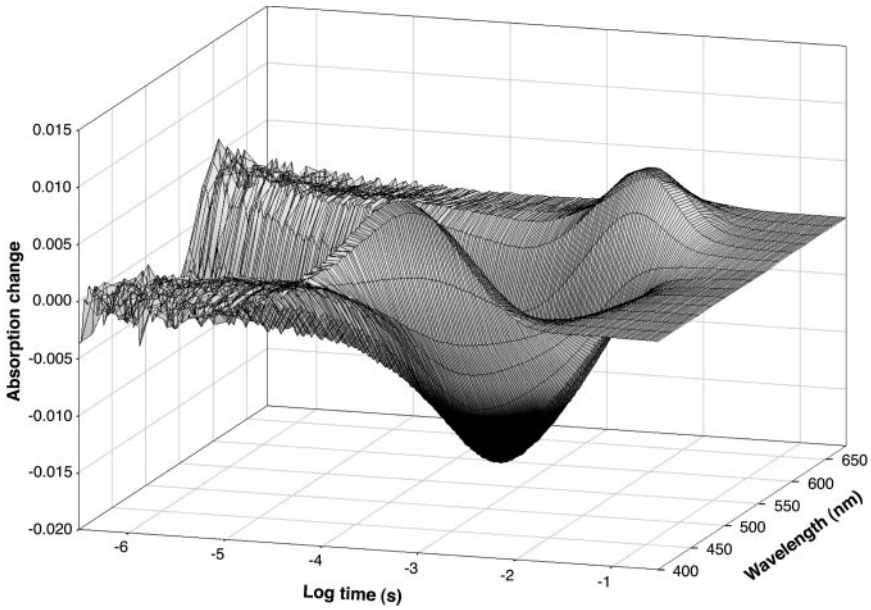

Fig. 2. Kinetics of light-induced absorption changes of wild-type LR in *N*-dodecyl-β-D-maltoside-treated *P. pastoris* membranes. Absorption changes taken at 20-nm intervals show a distinct BR-like character, with the fast photocycle ending well before 100 ms after the excitation. The fast photocycle is characteristic for ion-transporting rather than photosensory rhodopsins (3). Global multiexponential analysis of the data confirmed the existence of K, L, M, N, and O intermediates visible from the raw spectra. Conditions were as follows. The LR membranes were encased in polyacrylamide gel and equilibrated with 0.1 M NaCl, 0.05 M MES, and 0.05 M sodium phosphate (pH 6.0).

and releases it back during the O decay (Fig. 3*b*), similar to BR at pH values lower than the pK_a of the proton-releasing complex (18). Additionally, the pH-dependence of the photocycle bore a striking resemblance to that of BR. The decay of the M intermediate, which is associated with reprotonation of the Schiff base, was virtually pH-independent below 6, but

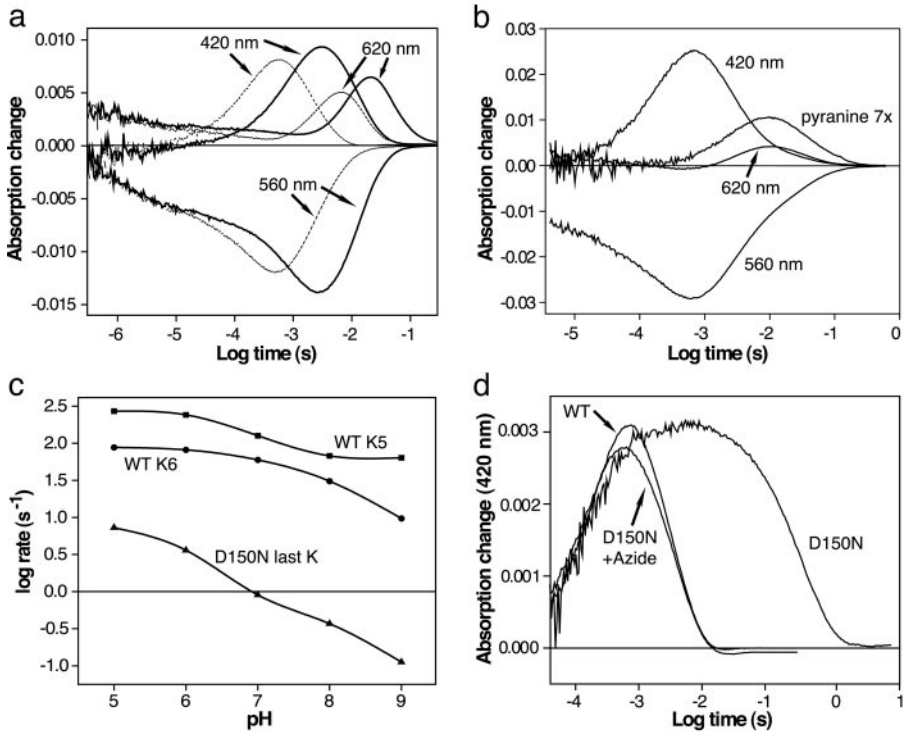

Fig. 3. Time-resolved spectroscopic analysis of LR. (*a*) Kinetic isotope effect on the photocycle. Conditions were the same as in Fig. 2 but with 0.01 M MES as a buffer with either H_2O (dotted lines) or D_2O (solid lines) as a solvent. (*b*) Kinetics of proton uptake and release in LR measured with pyranine (180 μM, magnified seven times) in unbuffered suspension of proton-permeable DMPC:DMPA liposomes. Liposomes were suspended in water with pH adjusted to 6.4 with NaOH and HCl. Upward deflection of the pyranine trace corresponds to proton uptake. (*c*) pH-dependence of the LR photocycle (wild-type and D150N mutant). The rates were obtained from multiexponential analysis of the data similar to those in *a* but taken at varying pH. Conditions were the same as in Fig. 2, but with 0.05 M 2-(*N*-cyclohexylamino)ethanesulfonic acid as a buffer at pH 9. The rates plotted for the wild-type correspond to the ultimate (middle curve, labeled K6) and the penultimate (upper curve, labeled K5) transitions, dominated by the O decay and M decay, respectively. The rate plotted for the D150N mutant corresponds to the last photocycle transition and is dominated by the M decay. The curves are drawn to guide the eye. (*d*) Kinetics of the Schiff base reprotonation in LR (M decay measured at 420 nm) demonstrating the cytoplasmic location of its proton donor. The mutation results in a 100-fold delay in the decay of M due to the lack of a primary Schiff base proton donor. Addition of sodium azide (10 mM) restores the M decay to rates comparable with the wild type. Conditions were the same as in Fig. 2.

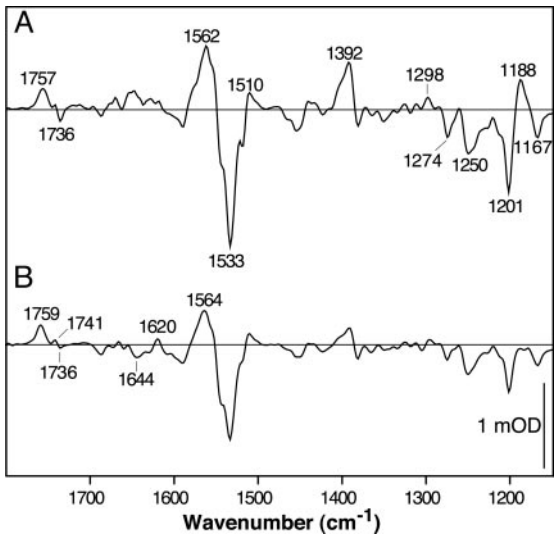

Fig. 4. Rapid-scan FTIR difference spectra of wild-type LR in DMPC:DMPA liposomes after laser photoexcitation demonstrating the changes of retinal and carboxylic acids under conditions of preferential accumulation of N (*A*) or M (*B*) intermediates (with minor contribution of O). Note the BR-like pattern of protonation, deprotonation, and perturbation of the carboxylic acids suggesting that the sequence and path of proton transfers is similar between LR and BR. Spectral resolution was 4 cm^{-1}, the traces were normalized by using a 1,757- to 1,759-cm^{-1} band. Conditions were as follows. The temperature was 0.5°C, the pH was 9 (*A*) or 8 (*B*), and the delay after excitation was 65 ms (*A*) or 10 ms (*B*).

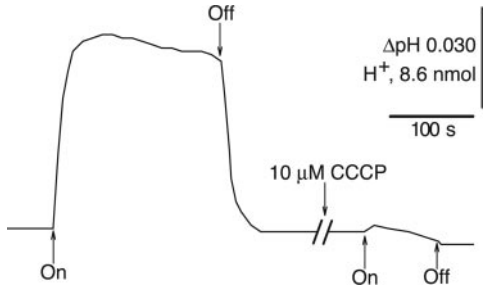

Fig. 5. Light-driven transmembrane transport of protons by wild-type LR incorporated into PC:PS liposomes suspended in 50 mM Na_2SO_4 and 50 mM K_2SO_4. The onset of illumination (>550 nm) is designated ''On'' with ''Off,'' indicating the end of illumination. Illumination causes rapid alkalinization of the medium, because of an influx of protons into the liposomes, with relaxation occurring once the light is removed. The pH of the suspension varied between 6.36 and 6.46 over the course of the measurements. A scale bar representing change in the proton concentration (calibrated with NaOH) and change in the actual pH of the medium is shown. Addition of 10 μM (final concentration) of the proton uncoupler CCCP abolishes the transport, indicating its primary character. The approximate amount of LR is 3 nmol per sample (2-ml volume).

became increasingly slow at higher pH values (Fig. 3*c*), resulting in decreased accumulation of O. This finding is indicative of an internal proton donor for the Schiff base with a pK_a of ≈7.5, similar to D96 in BR (19).

Rapid-scan FTIR difference spectroscopy confirmed the BR-like character of the LR photocycle. The data show pH- and temperature-dependent mixtures of M, N, and O intermediates, with all major retinal and carboxylic acid vibrational bands similar to those of BR (20). Of critical importance to the proton transfer mechanism, we saw protonation of a carboxylate reminiscent of BR's D85 (presumably D139), with the band downshifting from 1,759 cm^{-1} in M to values a few cm^{-1} lower in N (Fig. 4). We also observed absorption changes that can be ascribed to perturbation of a homolog of D115 (D179, +1,741 cm^{-1}/−1,736 cm^{-1}). More importantly, concomitant with accumulation of the N intermediate, we see transient deprotonation of a carboxylic acid at ≈1,736 cm^{-1} that resembles the band of the Schiff base proton donor in BR (D96) and may belong to D150 in LR. This finding is in contrast to what was observed for NR in which the perturbation of a homolog of D115 was in the opposite direction and the transient deprotonation of a homolog of D96 was not observed (6, 21).

These spectral and kinetic features suggest the BR-like pattern of proton transfers, where the Schiff base deprotonates to the extracellular side and is reprotonated from the cytoplasmic side, resulting in net transmembrane proton translocation. To confirm vectoriality of the transport, we replaced a putative Schiff base proton donor D150 with asparagine. In BR, lack of the cytoplasmic proton donor in the homologous mutant (D96N) results in a dramatic pH-dependent delay of the M-intermediate decay (22). In LR (Fig. 3*d*), we saw a similar delay (up to 100-fold) across all pH values measured (Fig. 3*c*), confirming that D150 is the cytoplasmic proton donor for the Schiff base. Such behavior is strikingly different from that in the homologous E142Q mutant of NR, where the Schiff base reprotonation rate is not affected (6). Sodium azide, known to function as a proton shuttle in hydrophobic regions of haloarchaeal rhodopsins (23, 24), restored the photocycle kinetics of the D150N mutant to rates comparable with the wild-type protein (Fig. 3*d*), similarly to the D96N mutant of BR. Additionally, the D150N mutation had minimal effect on the rate of M formation; therefore, the Schiff base deprotonation must occur toward the extracellular side.

The photocycle and proton kinetics of the wild-type and D150N LR strongly suggest that LR should act as a light-driven proton pump. To test whether any proton pumping does occur, we reconstituted solubilized purified LR into PC:PA, or PC:PS, or PC:CL liposomes. Constant illumination ($\lambda > 550$ nm) of an unbuffered proteoliposome suspension lead to an alkalinization of the medium up to 0.1 pH units (Fig. 5), which fully reversed in the dark. Addition of the proton uncoupler carbonylcyanide-3-chlorophenylhydrazone (CCCP) to the medium abolished these light-induced pH changes, with only a small step-like signal remaining. We believe this residual signal corresponded to the transient photostationary accumulation of late photocycle intermediates that gained a proton through the reprotonation of D150, consistent with the proton kinetics measured (Fig. 3*b*). Such light-dependent pH changes in the proteoliposome suspensions argue for active proton pumping with the BR-like orientation of LR (preferentially inside-out) (25). To evaluate the stoichiometry of proton pumping we estimated the buffering capacity and the protein content of the liposome system and obtained a value of 1–10 protons per second per LR molecule under nearly saturating light conditions. This finding is in a good accord with the photocycle turnover measured for similar proteoliposomes and implies relatively uniform orientation of LR, assuming the BR-like stoichiometry of one proton per cycle. Additionally, we tested the light-driven proton pumping of LR by following the absorbance changes of pyranine trapped inside the liposomes (25). We observed the light-induced reversible decrease in the amplitude of the visible band of pyranine absorbance (457 nm) corresponding to acidification of the internal volume of the liposomes. Addition of CCCP abolished this effect, confirming the active light-induced transport of protons into the LR liposomes.

In summary, we have provided direct experimental evidence for the activity of a retinal-based light-driven transmembrane proton pump from a eukaryote. This finding potentially reveals

a new pathway by which eukaryotes can build transmembrane proton gradients. At this point, we do not know how widespread this pathway may be. Even though >20 BR-like proteins are known for eukaryotes (26), some of them may serve as photosensors rather than ion pumps. It should be noted that the physiological role of the fungal light-driven proton pump need not be exclusively bioenergetic. For example, light-induced acidification of some cell compartments could be used to activate certain biochemical responses. In this respect, cellular localization of LR is a very interesting question, with mitochondria being an intriguing possibility. Despite these questions, we have nevertheless established the fact that fungi, similarly to prokaryotes, possess fast-cycling, retinal-based proton pumps in addition to slow-cycling sensory rhodopsins.

We thank Alex Idnurm and Barbara J. Howlett for providing DNA for the *Leptosphaeria ops* gene, Doreen E. Culham and Janet M. Wood for assistance in subcloning and mutating *ops* gene, Gerry Prentice for technical assistance, and Jacek Lipkowski for use of the Raman spectrometer. This work was supported by the Canada Foundation for Innovation/Ontario Innovation Trust, the Natural Sciences and Engineering Research Council of Canada, the Premier's Research Excellence Award, Research Corporation, and the University of Guelph.

1. Oesterhelt, D. & Stoeckenius, W. (1973) *Proc. Natl. Acad. Sci. USA* **70,** 2853–2857.
2. Béjà, O., Spudich, E. N., Spudich, J. L., Leclerc, M. & DeLong, E. F. (2001) *Nature* **411,** 786–789.
3. Spudich, J. L., Yang, C., Jung, K. & Spudich, E. N. (2000) *Annu. Rev. Cell Dev. Biol.* **16,** 365–392.
4. Saranak, J. & Foster, K. W. (1997) *Nature* **387,** 465–466.
5. Bieszke, J. A., Braun, E. L., Bean, L. E., Kang, S., Natvig, D. O. & Borkovich, K. A. (1999) *Proc. Natl. Acad. Sci. USA* **96,** 8034–8039.
6. Brown, L. S., Dioumaev, A. K., Lanyi, J. K., Spudich, E. N. & Spudich, J. L. (2001) *J. Biol. Chem.* **276,** 32495–32505.
7. Sineshchekov, O. A., Jung, K. H. & Spudich, J. L. (2002) *Proc. Natl. Acad. Sci. USA* **99,** 8689–8694.
8. Nagel, G., Ollig, D., Fuhrmann, M., Kateriya, S., Musti, A. M., Bamberg, E. & Hegemann, P. (2002) *Science* **296,** 2395–2398.
9. Idnurm, A. & Howlett, B. J. (2001) *Genome* **44,** 167–171.
10. Howlett, B. J., Idnurm, A. & Pedras, M. S. (2001) *Fungal Genet. Biol.* **33,** 1–14.
11. Bieszke, J. A., Spudich, E. N., Scott, K. L., Borkovich, K. A. & Spudich, J. L. (1999) *Biochemistry* **38,** 14138–14145.
12. Furutani, Y., Bezerra, A. G., Jr., Waschuk, S., Sumii, M., Brown, L. S. & Kandori, H. (2004) *Biochemistry* **43,** 9636–9646.
13. Aton, B., Doukas, A. G., Callender, R. H., Becher, B. & Ebrey, T. G. (1977) *Biochemistry* **16,** 2995–2999.
14. Kakitani, H., Kakitani, T., Rodman, H., Honig, B. & Callender, R. (1983) *J. Phys. Chem.* **87,** 3620–3628.
15. Gergely, C., Zimányi, L. & Váró, G. (1997) *J. Phys. Chem. B* **101,** 9390–9395.
16. Sasaki, J. & Spudich, J. L. (2000) *Biochim. Biophys. Acta* **1460,** 230–239.
17. Grzesiek, S. & Dencher, N. A. (1986) *FEBS Lett.* **208,** 337–342.
18. Zimányi, L., Váró, G., Chang, M., Ni, B., Needleman, R. & Lanyi, J. K. (1992) *Biochemistry* **31,** 8535–8543.
19. Balashov, S. P., Lu, M., Imasheva, E. S., Govindjee, R., Ebrey, T. G., Othersen, B., III, Chen, Y., Crouch, R. K. & Menick, D. R. (1999) *Biochemistry* **38,** 2026–2039.
20. Zscherp, C. & Heberle, J. (1997) *J. Phys. Chem. B* **101,** 10542–10547.
21. Bergo, V., Spudich, E. N., Spudich, J. L. & Rothschild, K. J. (2002) *Photochem. Photobiol.* **76,** 341–349.
22. Otto, H., Marti, T., Holz, M., Mogi, T., Lindau, M., Khorana, H. G. & Heyn, M. P. (1989) *Proc. Natl. Acad. Sci. USA* **86,** 9228–9232.
23. Lanyi, J. K. (1986) *Biochemistry* **25,** 6706–6711.
24. Tittor, J., Soell, C., Oesterhelt, D., Butt, H. J. & Bamberg, E. (1989) *EMBO J.* **8,** 3477–3482.
25. Seigneuret, M. & Rigaud, J. L. (1985) *FEBS Lett.* **188,** 101–106.
26. Brown, L. S. (2004) *Photochem. Photobiol. Sci.* **3,** 555–565.